Ukrainian Journal of Physical Optics
ISSUE 3
2024

Turbulence Image Recovery Based on Improved Generative Adversarial Networks

Bin Wei [1*], Houbu Li [1], Nan Ding [1], Shi Zhaoyang [2], Zhao Enguo [2**], Tao Rong [3], Fang Yao [3]

[1] CNPC Tubular Goods Research Institute, No.89 Jinye Second Road, Xi'an Shaanxi Province, China 710077, *e-mail: weibin06@cnpc.com.cn
[2] Shanghai Bojoe Sensing Technology Company Limited, Room 5, No.999 Jiangyue Road, Shanghai City, China 201114, **e-mail: 282833881@qq.com
[3] University of Shanghai for Science and Technology, No.516 Jungong Road, Shanghai City, China 2000093

Received: 07.04.2024

Abstract. In remote sensing systems, astronomical observations, traffic monitoring, and other medium- and long-range imaging systems, atmospheric turbulence caused by inhomogeneities in temperature, wind speed, humidity, etc., causes distortion when light waves propagate through the air. This leads to deterioration of image quality, its degradation, such as geometric deformation, blurring, etc. At the same time, a lot of useful information is lost. Therefore, it is important to effectively restore degraded images. In this paper, we propose an image recovery method based on an improved generative adversarial network (DeblurGAN-v2-CBAM), which is based on the DeblurGAN-v2 network and incorporates a convolutional attention module (CBAM) in the network to improve the network recovery image quality. Experimental results show that compared with DeblurGAN-v2 and SpA GAN models, the restoration quality of turbulence-corrupted image based on DeblurGAN-v2-CBAM network model has better performance with PSNR improvement of 0.6833 and SSIM improvement of 0.0118, effectively reducing the degree of blurring and geometric distortion of images.

Keywords: image recovery distorted by turbulence, generative adversarial networks, convolutional attention module
UDC: 004, 532.7, 535.2
DOI: 10.3116/16091833/Ukr.J.Phys.Opt.2024.03040

1. Introduction

Atmospheric turbulence is caused by random changes in atmospheric wind speed, air convection, inhomogeneous temperature, and pressure, which in turn cause random changes in atmospheric density. This can affect the images obtained by cameras used for street monitoring, astronomical observations, remote sensing, etc. The atmospheric refractive index changes randomly when light passes through the atmosphere due to the air's random motion. This distorts the wavefront phase and amplitude of the received light waves and destroys the original spatial and phase relationships, resulting in deformation and blurring of the target image. This seriously affects the feature recognition and information extraction of the target image, and the quality of the imaging is seriously degraded so that no adequate information can be obtained from the degraded image. This makes long-range observation, target identification, precise positioning, and target tracking challenging to achieve [1]. Therefore, recovering degraded images caused by atmospheric turbulence and improving image quality are of great practical importance.

Deep learning-based image restoration algorithms are widely used in computer vision tasks such as super-resolution reconstruction, image denoising, and deblurring. These algorithms have achieved good results. In 2014, Xu [2] et al. used deep convolutional neural networks to capture degraded features and the captured degraded features to recover potentially clear images from the degraded images. In 2015, Hradis [3] et al. found that convolutional neural networks can recover highly structured data successfully. In 2016, Mao [4] et al. constructed a very deep convolutional encoder-decoder network for image reconstruction using a symmetric jump connection method, which significantly improved the generalization ability of the neural network by cross-linking and deeper network layers. Still, the technique suffers from redundancy of network parameters, reduced computational speed, and overfitting. In 2017, Zhang [5] et al. removed the noise in the gradient domain by training a complete convolutional neural network (FCNN) and used the learned gradient method to guide the image deconvolution. In 2017, Nah [6] et al. proposed a multi-scale convolutional neural network that recovered clear images from various blurred images in an end-to-end manner. In 2018, Zhang [7] et al. used a trainable spatial variant, Recurrent Neural Networks (RNN), for blurred image recovery in dynamic scenes. The method achieved good results in the recovery of single dynamic blurred images. Still, it isn't easy to achieve satisfactory results for blurred images with complex spatial distribution (e.g., degraded atmospheric turbulence images). In 2019, Gao [8] et al. built an end-to-end supervised convolutional neural network (CNN) to reconstruct turbulence-damaged video sequences, and experiments showed that the proposed method could simultaneously deblur the video sequences, remove ripple effects, and enhance contrast. In recent years, many algorithms have used Generative Adversarial Networks (GAN) to recover images. In 2019, O. Kupyn [9] et al. proposed a new end-to-end generative adversarial network for individual image motion deblurring called DeblurGAN-v2, which can significantly improve deblurring efficiency, quality, and flexibility. In 2021, Lau [10] et al. proposed a GAN-based single-frame recovery algorithm to deal with turbulence-induced image distortion and blurring. In the same year, Jin [11] et al. proposed to generate an adversarial network TSR-WGAN for turbulence image recovery. Generative adversarial networks further improve image restoration, using generative adversarial network models to remove geometric distortions and recover high-quality images, offering the possibility of solving turbulent image restoration problems.

This paper proposes an improved generative adversarial network (DeblurGAN-v2-CBAM) to recover turbulent images. A feature pyramid network (FPN) structure for the generator is used for feature fusion to ensure better generation quality, and a convolutional block attention module (CBAM) is incorporated into the network. CBAM combines two modules: channel attention and spatial attention. Given a feature map, the attention weights are sequentially inferred along the spatial and channel dimensions and then multiplied with the original feature map to adaptively adjust the features. CBAM is a lightweight module that does not add overhead to the network. In this paper, according to the method proposed in the literature [12], a time-varying atmospheric turbulence degradation data set was constructed based on the Google Landmarks Dataset v2 data set [13] for training, and the improved network was verified to be feasible and effective.

2. Basic principles

2.1. Atmospheric-turbulence degradation model

The effects of atmospheric-turbulence degradation [14] mainly include turbulence-distortion operators and optical blur of sensors. The mathematical model describing the process of turbulence degradation is as follows [15]:

$$H(u) = G\left[D_u\left(I(u)\right)\right] + \varepsilon_u\,, \tag{1}$$

where $I(u)$ is the clear image; $H(u)$ is the turbulence-degraded image obtained by imaging equipment; $u = (xy)^T$ is the spatial location of pixels in an image; G is the sensor's optical blurring operator; D_u is the turbulence-distortion operator, which includes local deformation and spatial ambiguity; And ε_u is additive noise[16]. As the turbulence distortion operator contains both blur and deformation kernels, the global information of the image needs to be sensed when using the network to extract pixel features to improve the information recovery in the blurred regions.

2.2. Generative adversarial network

A generative adversarial network (GAN) [17] consists of two convolutional neural networks, a generator (*G*) and a discriminator (*D*). The basic model is shown in Fig. 1.

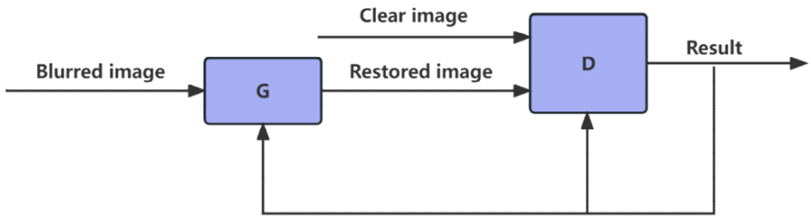

Fig. 1. Basic model for generating an adversarial network.

GAN is a new unsupervised architecture. *G* needs to generate an image that is infinitely close to the real image. *D* continuously improves its ability to discriminate between true and false by learning from a large number of positive and negative samples and obtaining the probability that the input image is the true image. *D* feeds the structure of the output to *G*, which uses it to adjust the parameters of the network so that more realistic samples can be generated later on. *D* will also train and learn in the process of continuous discrimination. Both sides are constantly competing and iterating, and both models are enhanced at the same time. *G* and *D* are trained simultaneously until Nash equilibrium is reached, at which point the resulting generator model is optimal. The objective function for GAN is shown in Eq. 2.

$$\min_G \max_D V(D,G) = E_{x\sim P(x)}\left[\log D(x)\right] + E_{z\sim P(z)}\left[\log\left(1 - D\left(G(z)\right)\right)\right] \tag{2}$$

where x is the true sample, $E_{x\sim P(x)}$ denotes the distribution of the true sample, z is random noise, $E_{z\sim P(z)}$ denotes that z obeys a certain distribution of noise, and $D(x)$ is the output of *D*, representing the probability that x is a true sample. $G(z)$ is the output of the *G*.

3. Improved convolutional attention module-based generative adversarial network

3.1. Network model of DeblurGAN-v2

DeblurGAN-v2 is an end-to-end generative adversarial network with improved image restoration efficiency and quality. G of DeblurGAN-v2 is framed by eeature pyramid networks (FPN) [9], which aggregates multiscale features instead of input multiscale features, with Inception-ResNet-v2 [18] as the backbone network. D uses a two-scale discriminator, using minimum mean square loss to evaluate on global and local scales, respectively. The network architecture of DeblurGAN-v2 is shown in Fig. 2. The turbulent degraded image is passed through the generator to get the recovered image, and the recovered image and the clear image are fed into the discriminator simultaneously. The global discriminator feeds the whole image, and the input of the local discriminator is a randomly cropped image block from the recovered image and the clear image. By calculating the loss, the network finally backpropagates the gradient update according to the loss result, and so on, until the generator generates the recovered image that is indistinguishable from the real one.

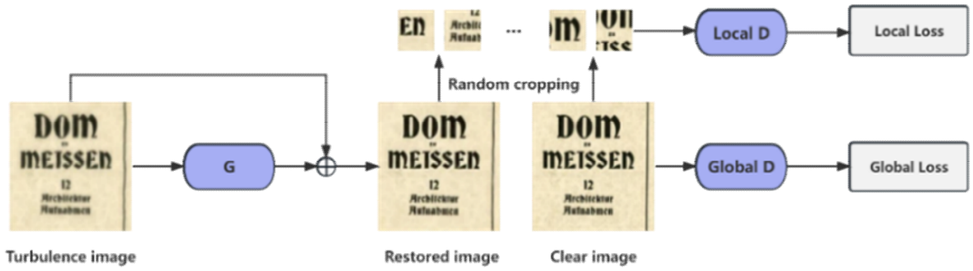

Fig. 2. Network architecture of DeblurGAN-v2.

Inspired by DeblurGAN-v2, this paper proposes an improved convolutional attention module-based generative adversarial network for the recovery of turbulent degraded images.

3.2. Improved DeblurGAN-v2 network structure

3.2.1. Generators. The generator of DeblurGAN-v2 uses the FPN framework and the backbone network uses the Inception-ResNet-v2 network. The generator's structure is shown in Fig. 3.

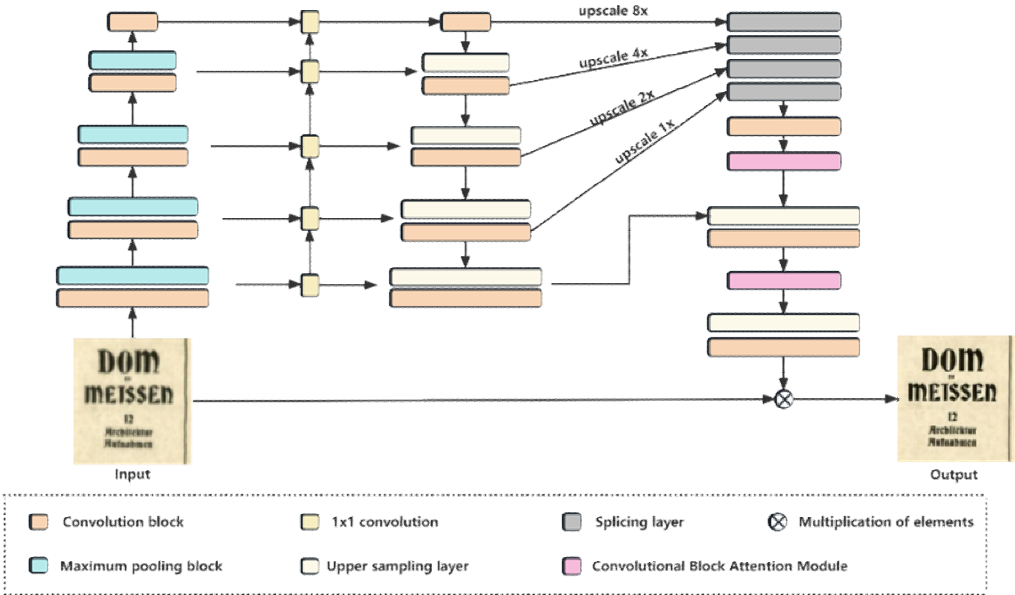

Fig. 3 Network structure of generators.

FPN includes bottom-up and top-down paths, as well as lateral connections. The bottom-up path is a convolutional network used for feature extraction, where images are down-sampled as they progress from bottom to top, allowing more semantic feature information to be extracted and compressed. The horizontal connections between the bottom-up and top-down channels complement the high-resolution detail and help locate objects. Five final feature maps of different scales are obtained from the FPN as the output. The output of the four feature maps is top-down and up-sampled to one-fourth of the input image size and concatenated into a tensor containing different levels of semantic information, fused with the feature map of the largest size. The up-sampling and convolution layers are added at the network's end to obtain a clear image. A jump connection from input to output is also introduced to fuse the obtained clear image with the original image to obtain the final recovered image, i.e., the recovered image generated by the generator.

To improve the quality of atmospheric turbulence degradation image recovery, the convolutional block attention module (CBAM) was incorporated into the network before the final up-sampling [19], and the improved network was named DeblurGANv2-CBAM. The CBAM module is a convolutional neural network module based on an attention mechanism for adaptive weighting and selecting features. The CBAM module consists of a channel and spatial attention modules. The channel attention module learns the interdependencies between each channel to weigh each channel adaptively. On the other hand, the spatial attention module learns the importance of different spatial locations and weights the feature maps to select the most essential features. CBAM is a lightweight module that does not add overhead to the network. the network structure of CBAM is shown in Fig. 4.

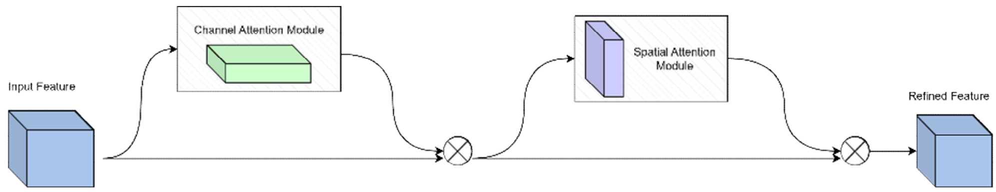

Fig. 4 Network structure of CBAM.

As shown in Fig. 5, the channel attention module takes the input feature maps F ($H \times W \times C$) for average and maximum pooling. Here, H, W, and C represent the height, width, and number of channels of the feature map, respectively, to obtain two of the features, and then feeds them into a shared multi-layer perception (MLP) with the number of neurons in the first layer as C / r (r is the reduction rate), the activation function as Relu, and the

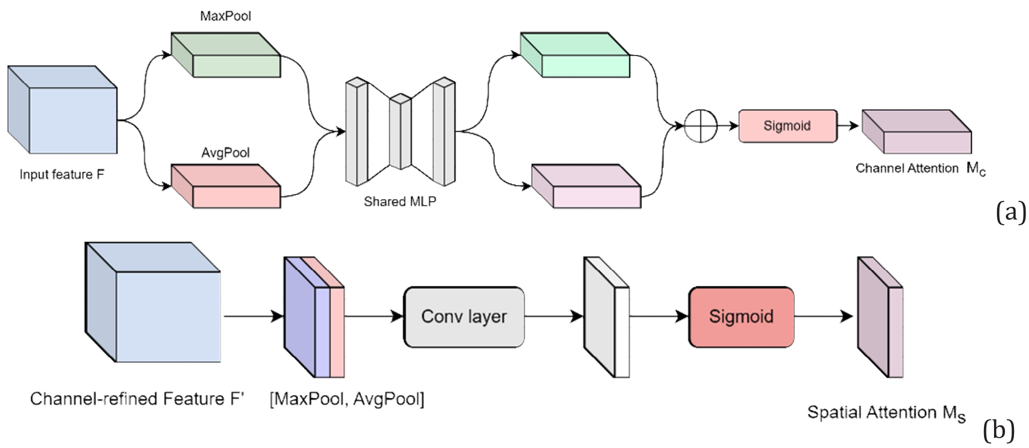

Fig. 5. Structure of channel and spatial attention module: (a) channel attention module, (b) spatial attention module.

number of neurons in the second layer as C. The output features of the MLP are summed and multiplied by the Sigmoid activation function to obtain the weight coefficients M_c. Multiplying M_c with F yields the input feature F' ($H \times W \times C$) for spatial attention. The spatial attention will perform maximum and average pooling with F' in the channel dimension to get two features ($H \times W \times 1$), and the two pooled results are stitched together by channel for 7×7 convolution operation. Then, the activation function is used to get the weight coefficients M_s. The CBAM feature map is obtained by multiplying M_s with F'.

3.2.2. Discriminators. The network's discriminator is the dual-scale discriminator of the DeblurGAN-v2 network, divided into a global and a local discriminator. The global discriminator discriminates the complete input image, and the local discriminator randomly crops the input image into image blocks and then discriminates them, which can prompt the generator to generate a more realistic recovered image during the backpropagation. The global and local discriminators in the dual-scale discriminator adopt the PatchGAN [20] structure, and the network structure is shown in Fig. 6.

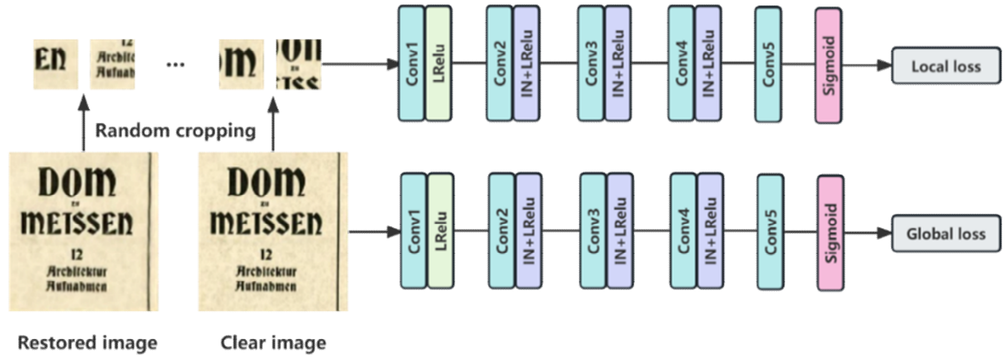

Fig. 6. Network structure of the discriminator.

Dual-scale discriminators are responsible for different dimensions of information. The global discriminator targets highly non-uniform blurring and integrates global contextual information, while the local discriminator extracts detailed information from the image. Combining these two discriminators facilitates the network to handle larger and more complex fuzzy types. The dual-scale discriminator yields two kinds of losses, global loss and local loss, which motivate the network to obtain the feature information of the image from different dimensions. The discriminator loss is defined as:

$$L_D = E_{x\sim P(x)}\left[\left(D(x) - E_{z\sim P(z)}D(G(z)) - 1\right)^2\right] + E_{z\sim P(z)}\left[\left(D(G(z)) - E_{x\sim P(x)}D(G(z)) + 1\right)^2\right]. \tag{3}$$

3.3. Loss function

The loss function incorporates three types of losses: pixel loss L_p, perceptual loss L_c, and adversarial loss L_D. L_p, L_c are content loss, and L_D is adversarial loss. Content loss focuses on recovering the main structure of the image, while adversarial loss focuses on recovering texture details, and the loss function L_G equation is as follows:

$$L_G = 0.5L_p + 0.006L_c + 0.01L_D, \tag{4}$$

where L_p is the pixel space loss, expressed using mean squared error (MSE), as shown in Eq. 5.

$$L_p = \frac{1}{N}\sum_{n=1}^{N} || C - S ||^2 , \tag{5}$$

where N denotes the number of data pairs for network training input, C is the generated image, and S is the corresponding original clear image, L_c is the perceptual loss [21], based on the CNN feature map difference between the generated image and the original clear image on VGG-19 [22]:

$$L_c = \frac{1}{W_{i,j}H_{i,j}}\sum_{x=1}^{W_{i,j}}\sum_{y=1}^{H_{i,j}}\left(\psi_{i,j}(C)_{x,y} - \psi_{i,j}(S)_{x,y}\right)^2 , \tag{6}$$

where $W_{i,j}$ and $H_{i,j}$ denote the dimensionality of the feature maps, and $\psi_{i,j}$ is the feature map obtained after activating of the *j*-th convolutional layer before the *i*-th maximum pooling layer in the VGG-19 network, pre-trained on ImageNet.

4. Experiment

In this paper, we use an NVIDIA GeForce RTX 3090 graphics card, a Windows system, PyTorch 1.12.1, and CUDA 11.6. During the network training process, Adam's optimization algorithm was utilized to optimize parameters. 50 epochs were trained, and the learning rate and Batch Size were set to 1 to ensure the network's stability.

This paper's data set uses the Google Landmarks Dataset v2 dataset and selects 100 images from it. According to the method proposed in the literature [12], a time-varying degraded image data set caused by atmospheric turbulence was constructed. 200 frames of turbulence degradation images were constructed for each image, which were RGB three-channel images of size 256×256. 12000 of these images were used as the training set, 4000 as the validation set, and 4000 as the test set. An example of the dataset is shown in Fig. 7.

Fig. 7. The data set of time-varying degraded images caused by atmospheric turbulence.

In this paper, subjective and objective evaluation methods are used to evaluate image quality. The subjective evaluation method mainly observes the visual effects of the reconstructed image. The objective evaluation methods mainly use the commonly used peak signal-to-noise ratio (PSNR) and Structure Similarity (SSIM) as the quality evaluation indexes of reconstructed images. PSNR is the maximum pixel value ratio to the mean square error. The larger the value, the smaller the distortion of the reconstructed image. Its calculation is shown in Eq. 7:

$$PSNR = 10 \times \log_{10}\left(\frac{MAX_I^2}{MSE}\right), \tag{7}$$

where MAX_I is the maximum value of image pixels. When given an original image I with size $m \times n$ and a noisy image K, the root mean square error formula is shown in Eq. 8:

$$MSE = \frac{1}{mn}\sum_{i=0}^{m-1}\sum_{j=0}^{n-1}|| I(i,j) - K(i,j)||^2 . \tag{8}$$

SSIM is an index to measure the similarity between two images, and its value range is [0,1]. The calculation of SSIM is shown in Eq. 9:

$$SSIM(Y,Y') = \frac{\left(2\mu_Y\mu_{Y'} + C\right)\left(2\sigma_{YY'} + C'\right)}{\left(\mu_Y^2 + \mu_{Y'}^2 + C\right)\left(\sigma_Y^2 + \sigma_{Y'}^2 + C'\right)}, \tag{9}$$

where Y and Y' represent the original high-resolution image and the reconstructed image, respectively; μ and σ represent the mean and variance of the image; $\sigma_{YY'}$ represents the covariance of the two images; C and C' are the normal numbers close to 0. The calculation of SSIM is based on image brightness, contrast and structure information. The larger the SSIM value, the higher the similarity between the two images.

5. Analysis of experimental results

In this paper, the DeblurGAN-v2 and SpA GAN [23] models are selected for comparative analysis with the improved DeblurGAN-v2-CBAM model, which is trained separately using a time-varying turbulent atmospheric degradation dataset in the same experimental setting, and the models are obtained and tested separately. The network model is evaluated by analyzing the image recovery effect, and the PSNR and SSIM metrics are used to objectively evaluate the recovery model. The average values of PSNR and SSIM are taken in the experiment. The results are shown in Table 1, from which it can be seen that the PSNR and SSIM of the improved DeblurGAN-v2-CBAM model in this paper are the highest, compared with DeblurGAN- v2, the PSNR is improved by 0.6833, and the SSIM is improved by 0.0118.

Table 1. Comparison of the recovery results of two images with degradation caused by turbulence.

Model	PSNR, dB	SSIM
DeblurGAN-V2	30.0035	0.9083
SpA GAN	23.5722	0.7808
DeblurGANv2-CBAM	30.6868	0.9201

The results of the generated recovered images are shown in Fig. 8, from left to right: the real clear image, the turbulence degraded image, the output image after the DeblurGAN-v2 model processing, the output image after the SpA GAN model processing, and the output image after the DeblurGANv2-CBAM model processing in this paper. The PSNR and SSIM calculated for each image for the clear image are shown below the image.

As can be seen in Fig. 8, the image deformation after DeblurGAN-v2-CBAM recovery is significantly improved. The deblurring effect is enhanced, the image is sharper, and the edge detail is also improved, which is closer to the real reference image. From an objective point of view, the PSNR and SSIM metrics of the DeblurGAN-v2-CBAM recovered images are also the highest, indicating that the network improvement is feasible.

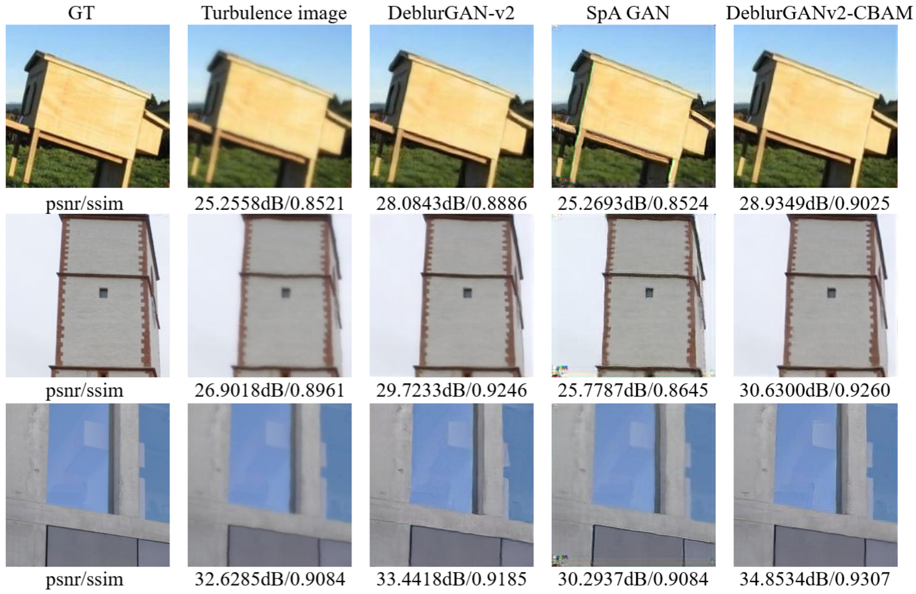

Fig. 8. Recovered images, whose degradation is caused by time-varying turbulence.

Fig. 9. Image restoration results in GOPRO dataset whose degradation is caused by time-varying turbulence.

To verify the generalization capability of our DeblurGANv2-CBAM network, we tested it on a GOPRO [24] dataset. Fig. 9 shows the restoration results of the DeblurGAN-v2 network and our improved DeblurGAN-v2-CBAM network on the GOPRO dataset. PSNR and SSIM indexes are used to evaluate the restoration model objectively. The first row represents the image after turbulence disturbance, the second row represents the image of turbulence degradation after restoration by the DeblurGAN-v2 network, and the third row represents the image of turbulence degradation after restoration by the DeblurGAN-v2-CBAM network. In the first column of the building scene, DeblurGAN-v2-CBAM can sufficiently suppress the blur and pixel displacement caused by turbulence, and the restored image highlights the edge outline of the building and critical information details. In the third column of turbulent image details of character scenes, the improved network restores the details of scenes and improves the visual quality of pictures. Our network can more accurately recover details and textures in turbulent blurred images, resulting in higher-quality restored images. In addition, DeblurGAN-v2-CBAM is also more robust to noise and other image artifacts. Therefore, DeblurGAN-v2-CBAM is a potential image restoration method suitable for image restoration in various turbulent environments and related fields.

6. Conclusion

In order to improve the recovery quality of degraded images caused by atmospheric turbulence, DeblurGAN-v2 is improved by incorporating a CBAM into the network, and the DeblurGAN-v2-CBAM network is proposed. The CBAM can adaptively weigh the features in the global and local range of the feature map to improve the representation capability and reduce redundancy, solve the information loss problem in the convolutional layer, and focus on key features, and the CBAM is a lightweight module that does not increase the overhead of the network. The experimental results show that compared with DeblurGAN-v2, the network model is enhanced for the recovery of degraded by turbulence images, with PSNR improved by 0.6833 and SSIM refined by 0.0118. The method can improve the image quality and solve the problem of object deformation in the images, and the recovered images have a higher resolution.

Funding

This work was supported by the National Natural Science Foundation of China (No. 62275153, 62005165), Shanghai Industrial Collaborative Innovation Project (HCXBCY-2022-006), the development fund for Shanghai talents (No:2021005), the Key Basic Research Projects of the Basic Strengthening Plan (Grant No. 2021-JCJQ-ZD040-02-03), the Key Laboratory of Space Active Opto-electronics Technology of Chinese Academy of Sciences (2021ZDKF4), and the Shanghai Science and Technology Innovation Action Plan (22dz1201300).

References

1. Shacham, O., Haik, O., & Yitzhaky, Y. (2007). Blind restoration of atmospherically degraded images by automatic best step-edge detection. *Pattern Recognition Letters*, *28*(15), 2094-2103.
2. Xu, L., Ren, J. S., Liu, C., & Jia, J. (2014). Deep convolutional neural network for image deconvolution. *Advances in neural information processing systems*, *27*.
3. Hradiš, M., Kotera, J., Zemcık, P., & Šroubek, F. (2015, September). Convolutional neural networks for direct text deblurring. In *Proceedings of BMVC* (Vol. 10, No. 2).
4. Mao, X., Shen, C., & Yang, Y. B. (2016). Image restoration using very deep convolutional encoder-decoder networks with symmetric skip connections. *Advances in neural information processing systems*, *29*.
5. Zhang, J., Pan, J., Lai, W. S., Lau, R. W., & Yang, M. H. (2017). Learning fully convolutional networks for iterative non-blind deconvolution. In *Proceedings of the IEEE Conference on Computer Vision and Pattern Recognition* (pp. 3817-3825).
6. Nah, S., Hyun Kim, T., & Mu Lee, K. (2017). Deep multi-scale convolutional neural network for dynamic scene deblurring. In *Proceedings of the IEEE conference on computer vision and pattern recognition* (pp. 3883-3891).
7. Zhang, J., Pan, J., Ren, J., Song, Y., Bao, L., Lau, R. W., & Yang, M. H. (2018). Dynamic scene deblurring using spatially variant recurrent neural networks. In *Proceedings of the IEEE conference on computer vision and pattern recognition* (pp. 2521-2529).
8. Gao, J., Anantrasirichai, N., & Bull, D. (2019). Atmospheric turbulence removal using convolutional neural network. *arXiv preprint arXiv:1912.11350*.
9. Kupyn, O., Martyniuk, T., Wu, J., & Wang, Z. (2019). Deblurgan-v2: Deblurring (orders-of-magnitude) faster and better. In *Proceedings of the IEEE/CVF international conference on computer vision* (pp. 8878-8887).
10. Lau, C. P., Lai, Y. H., & Lui, L. M. (2019). Restoration of atmospheric turbulence-distorted images via RPCA and quasiconformal maps. *Inverse Problems*, *35*(7), 074002.
11. Jin, D., Chen, Y., Lu, Y., Chen, J., Wang, P., Liu, Z., Guo, S.& Bai, X. (2021). Neutralizing the impact of atmospheric turbulence on complex scene imaging via deep learning. *Nature Machine Intelligence*, *3*(10), 876-884.

12. Mao, Z., Chimitt, N., & Chan, S. H. (2021). Accelerating atmospheric turbulence simulation via learned phase-to-space transform. In *Proceedings of the IEEE/CVF International Conference on Computer Vision* (pp. 14759-14768).
13. Weyand, T., Araujo, A., Cao, B., & Sim, J. (2020). Google landmarks dataset v2-a large-scale benchmark for instance-level recognition and retrieval. In *Proceedings of the IEEE/CVF conference on computer vision and pattern recognition* (pp. 2575-2584).
14. Xie, Y., Zhang, W., Tao, D., Hu, W., Qu, Y., & Wang, H. (2016). Removing turbulence effect via hybrid total variation and deformation-guided kernel regression. *IEEE Transactions on Image Processing*, *25*(10), 4943-4958.
15. Chan, S. H. (2022). Tilt-then-blur or blur-then-tilt? clarifying the atmospheric turbulence model. *IEEE Signal Processing Letters*, *29*, 1833-1837.
16. Xu, B., Fang, Y., Zhang, L., Zhang, D., & Zheng, L. (2023). Turbulent-image Restoration Based on a Compound Multibranch Feature Fusion Network. *Current Optics and Photonics*, *7*(3), 237-247.
17. Goodfellow, I., Pouget-Abadie, J., Mirza, M., Xu, B., Warde-Farley, D., Ozair, S., Courville, A. & Bengio, Y. (2014). Generative adversarial nets. *Advances in neural information processing systems*, *27*.
18. Szegedy, C., Ioffe, S., Vanhoucke, V., & Alemi, A. (2017, February). Inception-v4, inception-resnet and the impact of residual connections on learning. In *Proceedings of the AAAI conference on artificial intelligence* (Vol. 31, No. 1).
19. Woo, S., Park, J., Lee, J. Y., & Kweon, I. S. (2018). Cbam: Convolutional block attention module. In *Proceedings of the European conference on computer vision (ECCV)* (pp. 3-19).
20. Li, C., & Wand, M. (2016). Precomputed real-time texture synthesis with markovian generative adversarial networks. In *Computer Vision–ECCV 2016: 14th European Conference, Amsterdam, The Netherlands, October 11-14, 2016, Proceedings, Part III 14* (pp. 702-716). Springer International Publishing.
21. Johnson, J., Alahi, A., & Fei-Fei, L. (2016). Perceptual losses for real-time style transfer and super-resolution. In *Computer Vision–ECCV 2016: 14th European Conference, Amsterdam, The Netherlands, October 11-14, 2016, Proceedings, Part II 14* (pp. 694-711). Springer International Publishing.
22. He, K., Zhang, X., Ren, S., & Sun, J. (2016). Deep residual learning for image recognition. In *Proceedings of the IEEE conference on computer vision and pattern recognition* (pp. 770-778).
23. Pan, H. (2020). Cloud removal for remote sensing imagery via spatial attention generative adversarial network. *arXiv preprint arXiv:2009.13015*.
24. Nah, S., Hyun Kim, T., & Mu Lee, K. (2017). Deep multi-scale convolutional neural network for dynamic scene deblurring. In *Proceedings of the IEEE conference on computer vision and pattern recognition* (pp. 3883-3891).

Bin Wei, Houbu Li, Nan Ding, Shi Zhaoyang, Zhao Enguo, Tao Rong, Fang Yao. (2024). Turbulence Image Recovery Based on Improved Generative Adversarial Networks**.** *Ukrainian Journal of Physical Optics*, *25*(3), 03040 – 03050.
doi: 10.3116/16091833/Ukr.J.Phys.Opt.2024.03040

Анотація*. У системах дистанційного зондування, при астрономічних спостереженнях, при моніторингу дорожнього руху та в інших систем отримання зображень на середніх та великих відстанях атмосферна турбулентність, спричинена неоднорідністю температури, швидкістю вітру, вологістю тощо, спричиняє спотворення, у випадку коли світлові хвилі поширюються в повітрі. Це призводить до погіршення якості зображення, його деградації, такій як геометрична деформація, розмиття тощо. При цьому втрачається багато корисної інформації. Тому важливо ефективно відновлювати погіршені зображення. У цій статті ми пропонуємо метод відновлення зображення на основі вдосконаленої генеративної змагальної мережі (DeblurGAN-v2-CBAM), яка базується на мережі DeblurGAN-v2 і включає в мережу згорткового блоку модуля уваги (CBAM) для покращення мережі і відновлення якості зображення. Експериментальні результати показують, що порівняно з моделями DeblurGAN-v2 і SpA GAN якість відновлення зображення пошкодженого внаслідок турбулентності на основі моделі мережі DeblurGAN-v2-CBAM має кращу продуктивність із покращенням PSNR на 0,6833 і покращенням SSIM на 0,0118, що ефективно знижує ступінь розмитість і геометричне спотворення зображень.*

Ключові слова*: відновлення зображення пошкодженого турбулентністю, генеративні змагальні мережі, згортковий блоку модуля уваги*